Prepared for submission to JCAP

arXiv:1207.4043v1 [astro-ph.HE] 17 Jul 2012

A Search for Correlation of Ultra-High Energy Cosmic Rays with IRAS-PSCz and 2MASS-6dF Galaxies

Foteini Oikonomou,[a,b] **Amy Connolly,**[c] **Filipe B. Abdalla**[a] **Ofer Lahav,**[a] **Shaun A. Thomas,**[a,b] **David Waters**[d] **and Eli Waxman**[e]

[a]Astrophysics Group, Department of Physics and Astronomy, University College London,
Gower Street, London WC1E 6BT, United Kingdom

[b]UCL - Institute of Origins, Faculty of Mathematical and Physical Sciences, University College London

[c]Department of Physics and CCAPP, The Ohio State University,
191 West Woodruff Avenue, Colombus, Ohio 43210, USA

[d]High Energy Physics Group, Department of Physics and Astronomy, University College London

[e]Department of Particle Physics & Astrophysics, Weizmann Institute of Science,
Rehovot 76100, Israel

E-mail: fotini@star.ucl.ac.uk

Abstract.
We study the arrival directions of 69 ultra-high energy cosmic rays (UHECRs) observed at the Pierre Auger Observatory (PAO) with energies exceeding 55 EeV. We investigate whether the UHECRs exhibit the anisotropy signal expected if the primary particles are protons that originate in galaxies in the local universe, or in sources correlated with these galaxies. We cross-correlate the UHECR angular positions with the positions of IRAS-PSCz and 2MASS-6dF galaxies (with median depth of 120 and 225 Mpc respectively) weighted for GZK and other particle propagation effects. This is the first time that the 6dF survey is used for a study of this type and the first time that the PSCz survey is used with the full 69 publicly released PAO events. We find the probability that the observed UHECR events are consistent with an isotropic hypothesis to be less than 5% for most of the parameter space considered. The observed correlation is consistent with the mean of the model distribution of UHECRs associated with PSCz and 6dF galaxies. The agreement in results between the two catalogues, which probe similar large scale structure, is very good. Finally, we explore how the random magnetic deflections of UHECRs during propagation affect the expected anisotropy signal.

Contents

1 Introduction 1

2 Methodology 3
- 2.1 The Pierre Auger observatory . . . 3
- 2.2 The 6 degree field galaxy survey . . . 4
- 2.3 The IRAS PSCz . . . 4
- 2.4 Model of UHECR source distribution . . . 5
- 2.5 Magnetic fields . . . 7
- 2.6 Correlation statistic . . . 8

3 Results 9
- 3.1 Cross-correlation of UHECRs and nearby LSS . . . 9
- 3.2 Magnetic deflection . . . 16

4 Discussion and Conclusions 17

5 Acknowledgements 18

Bibliography 18

1 Introduction

The origin of cosmic rays (CRs) with energies exceeding 10 EeV (1 EeV = 10^{18} eV) remains unknown despite decades of extensive research. Such particles are referred to as ultra-high energy cosmic rays (UHECRs) and their sources are probably extra-galactic [1], [2]. Their gyro-radius is larger than could be contained in the magnetic field of our galaxy [3].

UHECRs with energy above ~ 50 EeV are above the threshold for pion photo-production upon collision with cosmic microwave background (CMB) photons, a process which was predicted soon after the discovery of CMB radiation, known as the GZK cutoff [4], [5]. The most recent published cosmic ray spectra measured by the High Resolution Fly's Eye (HiRes), PAO and Telescope Array (TA) experiments confirm this cutoff in the CR spectrum [6], [7], [8]. As a result of the GZK process UHECRs that arrive on earth with energy exceeding 50 EeV must originate in sources within a few hundred mega-parsecs (Mpc).

Only a handful of known astrophysical populations are likely to have the required power to accelerate CRs to such high energies [3], [9]. The most likely candidates are active galactic nuclei (AGN) and gamma ray bursts (GRBs) (see however [10], [11], [12] for a recent result and alternative interpretations on GRBs as UHECR sources).

If extra-galactic magnetic fields (EGMFs) are not too large, UHECRs must point back to their sources within a few degrees if they are protons, due to their high rigidity. Hence if they originate in some astrophysical population, the arrival direction distribution of UHECRs should be correlated with that population as well as with the distribution of large scale structure (LSS) in the local universe, since matter in the Universe is clustered [13]. An isotropic arrival direction distribution of UHECRs could indicate either a heavier composition or new physics such as heavy relic particles (see [1] for a review of experimental signatures).

Besides the origin, another question which remains open is the composition of UHECRs. The PAO, the largest UHECR observatory to date, has not reported on the composition of UHECRs with energy exceeding 20 EeV, presumably due to the small number of observed events. Their most recent results between $1-20$ EeV suggest that there is a smooth transition from light, proton-like to heavier, Fe-like nuclei [14]. It should be noted that HiRes and TA results up to an energy of 50 EeV agree with a proton-like composition [15], [16]. There are a number of reasons why one wouldn't expect heavy nuclei at energies above the GZK threshold (see for example [17]) not least that the leading extra-galactic candidate sources are expected to accelerate primarily protons.

In this work we revisit the question of the origin of UHECRs, following the release of the arrival directions of 69 UHECRs with energy above 55 EeV recorded up until December 2009 by the PAO [18]. We model the local UHECR source distribution using galaxy catalogues of the nearby universe. The 6 degree Field Galaxy survey (6dF) is being used in this paper for the first time to derive the expected UHECR source distribution. The IRAS Point Source Catalogue of redshifts (PSCz), although previously used for cross correlations with UHECRs (see references below), is being used here for the first time to analyse the updated dataset of 69 observed UHECRs. We refrain from imposing any artificial distance cuts on potential UHECR sources and instead introduce a weighting system which ensures that the expected contribution of distant sources to the UHECR flux on earth drops off naturally with distance. We also investigate the effect of random magnetic deflections on any correlation between the source population and the observed UHECR arrival direction distribution.

A number of authors have looked for the sources of UHECRs in the past, by cross-correlating the observed arrival directions with the positions of nearby galaxy catalogues, in particular the PSCz [19], [20], [21], [22], [23], 2MRS [24], [18], [25] and others with the positions of specific classes of objects, AGN [26], [27], [28], [29], [30], BL LAcs [31] and LIRGs [20] among others, reporting different degrees of correlation depending on the UHECR sample, statistical approach and source population used. The authors of [19] analysed the arrival directions of 27 UHECRs with energy above 55 EeV detected until August 2007 and found that the UHECRs exhibited a stronger correlation with propagation weighted PSCz galaxies than 99.8% of isotropic realisations. The authors of [24] analysed the distribution of the 69 observed UHECRs and found that 21 of the 55 that survive their cuts correlate with nearby AGN. The probability of finding such a correlation assuming isotropy is 0.003. Further they cross-correlated the arrival directions of the UHECRs with the positions of 2MRS galaxies and Swift-BAT X-ray sources [32]. For the values of the free parameters in their models that maximise the likelihood they found that the fraction of isotropic realisations that yield a higher likelihood than the observed UHECRs are 0.004 and 2×10^{-4} for the 2MRS and Swift-BAT respectively. The results they obtained are *a posteriori* and do not constitute a confidence level on anisotropy. Because of the different approaches followed their results are not directly comparable to ours.

This work is organised as follows. In Section 2 we present the formalism used to analyse the arrival direction distribution of UHECRs, in Section 3 we present our main results applied to the measured PAO data and in Section 4 we discuss the implications of our results and conclude.

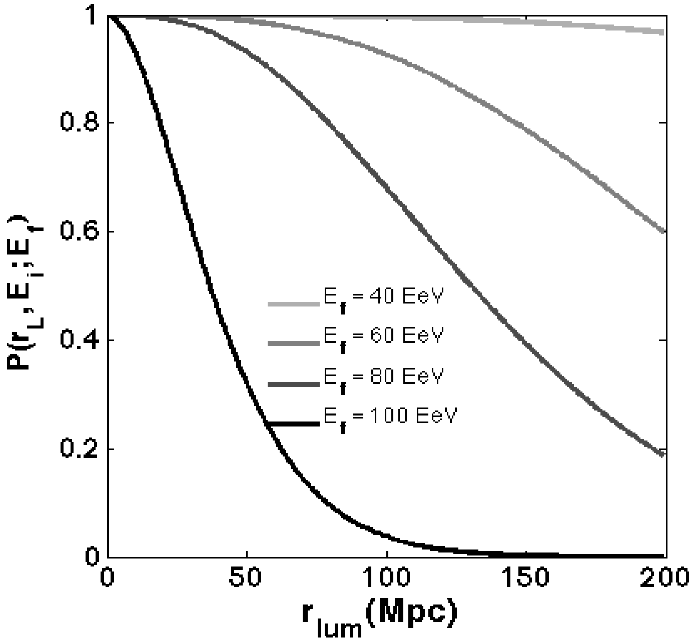

Figure 1: The function $P_p(r_L, E_i; E_f)$, which represents the probability that a UHECR emitted at a source at luminosity distance r_L, with initial energy E_i, will be observed with final energy above E_f, here shown as a function of propagation distance for $E_i = 200$ EeV and $E_f \geq 40, 60, 80, 100$ EeV.

2 Methodology

We study the correlation between the arrival directions of the 69 PAO observed events (§2.1) and the distribution of matter in the local LSS which we model using the 6dF (§2.2) and the PSCz (§2.3) catalogues. In §2.4 we present our models of UHECR source distribution. Throughout this analysis we take into account the non-uniform PAO exposure (§2.1). In §2.5 we explain our treatment of the expected UHECR random magnetic deflections. In §2.6 we present our statistical approach.

2.1 The Pierre Auger observatory

The PAO, in Malargue Argentina is a cosmic ray observatory dedicated to the detection of cosmic rays of energy greater than of 1 EeV. Data taking started in January 2004 and since then the arrival direction and reconstructed energy of 69 UHECRs exceeding 55 EeV have been published. At the PAO, which has a detection area of 3000 km^2, UHECR particle showers are detected by 1600 ground based Cherenkov detectors surrounded by 24 fluorescence telescopes, which measure the amount of energy dissipated in the atmosphere in the form of ultra-violet radiation [33]. The combination of these two techniques provides the most accurate reconstruction of UHECR shower geometry to date. Full time operation ensures an exposure which is uniform in right ascension and fully efficient for zenith distance up to $\theta_m = 60°$. The PAO exposure is a function of declination and is given by [34]:

$$\omega(\delta) \propto \cos(a_0)\cos(\delta)\sin(\alpha_m) + \alpha_m \sin(a_0)\sin(\delta), \tag{2.1}$$

where δ is the declination and a_0 is the latitude of the PAO which is $-35.2°$. Here, α_m is given by:

$$\alpha_m = \begin{cases} 0 & \text{if } \xi > 1 \\ \pi & \text{if } \xi < -1 \\ \cos^{-1}(\xi) & \text{otherwise} \end{cases}$$

and

$$\xi \equiv \frac{\cos(\theta_m) - \sin(a_0)\sin(\delta)}{\cos(a_0)\cos(\delta)}.$$

The PAO has an integrated exposure of $\sim$ 20000 km^2 year and $\sim$ 20 UHECRs above the GZK threshold are detected every year since its completion in November 2008 [35].

2.2 The 6 degree field galaxy survey

The 6dF is a redshift and peculiar velocity survey of 2MASS selected galaxies which was carried out using the Six-Degree Field instrument on the Schmidt Telescope of the Anglo-Australian Observatory [36]. The survey, which covers the entire Southern Sky (excluding the Galactic plane, $|b| > 10°$), resulted in a catalogue of 125,071 galaxies and 110,256 associated redshifts. The 6dF has a median redshift $\overline{z} = 0.053$ which corresponds to a comoving distance of 225 Mpc for a flat universe with $\Omega_M = 0.25$, $\Omega_\Lambda = 0.75$ and $H_o = 70$ km s^{-1} Mpc^{-1}, which we assume throughout this work. The 6dF field of view covers 80% of the PAO field of view by area. Taking into account the total declination dependent PAO acceptance (equation 2.1) which is smaller for positive declinations, it covers 86.2% of the instantaneous PAO exposure. The 6dF is near-infrared selected, which means it favours older, bulge-dominated galaxies and therefore it is minimally affected by dust extinction. In this work the final 6dF data release [36] is being used for the first time for a study of the origin of high energy particles.

2.3 The IRAS PSCz

The PSCz is a redshift catalogue of infrared selected IRAS galaxies which covers 84% of the sky [37]. It contains 14,677 galaxies with associated redshifts, and median redshift ($\overline{z} = 0.028$) which corresponds to a comoving distance of 119 Mpc in the cosmological model we are assuming. Since the galaxies in the PSCz are infrared selected there is a preference for young, star-forming galaxies in the catalogue.

We have chosen to use two complementary galaxy surveys to derive the expected UHECR source distribution. The PSCz is a shallow nearly full-sky galaxy survey and its use facilitates comparison with results of previous studies. The 6dF on the other hand is a much larger survey ($\sim$ 20 times more galaxies than the PSCz in the southern hemisphere). The different median depths of the 2 surveys mean that they highlight different structures of the nearby universe (for example the Shapley Concentration (centred at ($l \sim -50°, b \sim 30°$) at a distance $\sim$ 200 Mpc is prominent in the 6dF) although there is a significant overlap. The 2 surveys consist of different galaxy populations with slightly different clustering properties. This means that they can be used to distinguish between different astrophysical populations as UHECR sources, although this is a subtle difference that will require a large UHECR dataset and a better understanding of UHECR magnetic deflections before it can be pursued.

2.4 Model of UHECR source distribution

We use the galaxy catalogues introduced above to model a UHECR source population which is steady and follows the distribution of luminous matter in the local universe. One of the parameters that our analysis is sensitive to is the density of UHECR sources. The uncertainty on the true position of the sources of observed UHECRs due to random magnetic deflections, means that groups of two or more UHECRs with arrival directions separated by less than a few degrees may have been produced by the same source and are referred to as repeaters. The number of repeaters in a dataset can constrain the density of sources of UHECRs [13], [38], [39]. We have searched for repeaters separated by less than 3°, intended to reflect the uncertainty associated with instrumental resolution ($\sim 1°$) and possible magnetic deflections of a few degrees (see §2.5), among the 69 observed PAO events. We found 9 doublets and 2 triplets, which suggests ~ 600 UHECR sources within the earth's GZK horizon and hence a source density $\sim 4 \cdot 10^{-4}$ Mpc^{-3}.

Here we consider a model in which the local number density of UHECR sources is comparable to that of galaxies in the local Universe ($\overline{n}_0 = 10^{-2}$ Mpc^{-3}) and UHECR sources are faint i.e. each source produces 1 or no events and the probability of a single source producing multiple events is low. If only one subtype of galaxy is responsible for the observed UHECR flux or the observed flux is dominated by a few "bright" sources (such as in models in which the nearby radio galaxy Centaurus A is responsible for much of the observed UHECR flux [40], [41], [42]) then the density of sources may be lower than considered here. More data will allow us to better constrain the UHECR source density. In our model we also assume that all UHECR sources are intrinsically identical.

We assign each galaxy in our model a weight, proportional to the expected UHECR flux from that source, which depends on the flux suppression with distance and the energy with which protons are emitted (this initial energy determines the energy losses during propagation due to interaction with background photons). The flux weight for a galaxy at luminosity distance r_L from earth that emits a cosmic ray proton with initial energy E_i which reaches the earth with energy equal to or greater than E_f, is given by:

$$\omega(r_L)_{\text{flux}} = \frac{1}{{r_L}^2} \int_{E_f}^{E_{\text{i,max}}} dE_i \int_{E_f}^{E_i} dE_f \, \rho_p(r_L, E_i; E_f) I(E_i), \tag{2.2}$$

where

$$\rho_p(r_L, E_i; E_f) = \left| \frac{\partial P_p(r_L, E_i; E_f)}{\partial E_f} \right|, \tag{2.3}$$

is the derivative of the function $P_p(r_L, E_i; E_f)$ which gives the probability of a proton arriving on earth with energy E_f if it was emitted with energy E_i by a source at distance r_L, introduced in [43]. For E_f we conservatively adopt the lowest measured energy (55 EeV) present in the PAO dataset. We set $E_{\text{i,max}}$ which is the maximum energy achievable through astrophysical processes equal to 10^{21} eV. The value of $E_{\text{i,max}}$ is not fully constrained by observations but considering higher values of $E_{\text{i,max}}$ would have a negligible effect on our results here, since UHECRs above this energy promptly interact with background photons. For the intrinsic spectrum of the UHECR sources $I(E_i, t)$ we consider a power law spectrum:

$$I(E_i) = I_0 E_i^{\alpha} \Theta(E_{\text{i,max}} - E_i). \tag{2.4}$$

The step function restricts the UHECRs to have energy below $E_{\rm i,max}$. Here I_0 normalises the injection spectrum such that:

$$\int_{E_f}^{E_{\rm i,max}} dE_i I_0 E_i^{\alpha} \Theta(E_{\rm i,max} - E_i) = 1. \tag{2.5}$$

We consider a power law with index $\alpha = -2$ which is what is expected in diffusive shock acceleration [44], [45]. We have investigated the sensitivity of our model to α and found that varying the value of α in the range $-2.5 \leq \alpha \leq -1.5$ has a negligible effect on our results. For the simulation of the proton propagation and energy losses we use the $\rho(r_L, E_i; E_f)$ function which was computed and made publicly available by the authors of [39] and [46] at `http://www.desy.de/~uhecr/P_proton`. In figure 1 we plot the function $P_p(r_L, E_i; E_f)$, which we obtain by numerically integrating over the $\rho(r_L, E_i; E_f)$ function, for UHECRs with $E_i = 200$ EeV and $E_f \geq 40, 60, 80, 100$ EeV.

To account for the effect of the flux limit of the survey on the observed number density of galaxies as a function of distance we need the survey's selection function, defined as the expected number density of galaxies in the survey as a function of distance, in the absence of clustering. One can model the selection function using a fit to the survey's redshift distribution, often parametrised as:

$$dN(z) = Az^{\beta} \exp\left[-\left(\frac{z}{z_p}\right)^{\gamma}\right] dz, \tag{2.6}$$

where A gives the normalisation, z_p the peak of the distribution and β, γ control the slope. All 4 parameters are specific to the survey (see [36] and [37] for 6dF and PSCz redshift distributions respectively). The overall selection function $\psi(r_c)$ is the redshift distribution divided by the volume element [47]:

$$\psi(r_c) = \frac{1}{\Omega_s r_c^2} \left(\frac{dN}{dz}\right)_{r_c} \left(\frac{dz}{dr_c}\right)_{r_c}, \tag{2.7}$$

where Ω_s is the solid angle of the survey and r_c the comoving distance. We weight the observed galaxy distribution by the inverse of $\psi(r_c)$ which we normalise to be 1 at $r_{min} =$ 5 Mpc comoving, so that the effective contribution of each survey galaxy to the model source distribution is:

$$\omega_{\rm gal} = \frac{\omega(r_L)_{flux}}{\psi(r_c)}. \tag{2.8}$$

Galaxy surveys measure redshifts not distances, and peculiar velocities along the line-of-sight affect our estimates of actual distances. The redshift of an object is defined by:

$$cz = H_0 r + (\mathbf{v}(\mathbf{r}) - \mathbf{v}(\mathbf{0})) \cdot \hat{\mathbf{r}}, \tag{2.9}$$

where $\mathbf{v}(\mathbf{r})$ is the object's peculiar velocity and $\mathbf{v}(\mathbf{0})$ is the observer's peculiar velocity. Working in a reference frame where $\boldsymbol{\Delta}\mathbf{v} = \mathbf{v}(\mathbf{r}) - \mathbf{v}(\mathbf{0})$ is small allows more accurate distance estimates. In the local universe, out to $cz \sim 3000$ kms^{-1}, where galaxies share the motions of the Local Group (LG) it is best to convert to the LG rest frame. Further away galaxy peculiar velocities are independent of the LG velocity and $\boldsymbol{\Delta}\mathbf{v}$ is smaller in the CMB rest frame. In this work we are interested in the distribution of matter nearby, hence it is most useful to work with LG frame redshifts. However we will also present our main results from redshifts in both frames.

To convert between cz_{Hel}, that is redshift measured in the heliocentric frame, and cz_{LG} we use the relation [48]:

$$cz_{LG} = cz_{\mathrm{Hel}} - 79\cos(l)\cos(b) + 296\sin(l)\cos(b) - 36\sin(b), \tag{2.10}$$

where l and b are the Galactic longitude and latitude respectively. To convert from the LG frame to the CMB frame we use:

$$cz_{CMB} = cz_{LG} + v_{LG}\left[\sin(b)\sin(b_{LG}) + \cos(b)\cos(b_{LG})\cos(|l_{LG} - l|)\right], \tag{2.11}$$

where v_{LG} is the amplitude of the LG velocity with respect to the CMB and (l_{LG}, b_{LG}) is the direction of its motion. Using the CMB dipole value obtained in [49] with 7 year data from WMAP we obtain $v_{LG} = 627$ km s^{-1} towards $(l_{LG} = 276^\circ, b_{LG} = 30^\circ)$.

2.5 Magnetic fields

A relativistic particle of energy E and charge Z in a magnetic field has a Larmor radius given by $r_{Lar} = \frac{E}{ZeB_\perp}$, where $B_\perp$ is the field strength in the direction perpendicular to the momentum of the particle. A relativistic proton in a field which is constant over a distance d will suffer a deflection

$$\theta(E,d) \approx \frac{d}{r_{Lar}} \approx \left(\frac{E}{100\ \mathrm{EeV}}\right)^{-1}\left(\frac{d}{1\ \mathrm{Mpc}}\right)\left(\frac{B_\perp}{10^{-9}\ \mathrm{G}}\right). \tag{2.12}$$

The strength and distribution of EGMFs are poorly known (see reviews of existing data in [50], [51]). Dense large scale structures such as galaxy clusters and galaxy filaments are likely to support relatively large magnetic fields whereas in between structures EGMFs are probably negligible. The deflection for a proton propagating a distance d through a magnetic field with r.m.s. strength B and coherence length λ is given by [52]:

$$\theta(E,d) \approx 0.05^\circ \left(\frac{d}{\lambda}\right)^{\frac{1}{2}}\left(\frac{\lambda}{10\ \mathrm{Mpc}}\right)\left(\frac{B}{10^{-11}\ \mathrm{G}}\right)\left(\frac{E}{100\ \mathrm{EeV}}\right)^{-1}. \tag{2.13}$$

The most realistic models of UHECR propagation through EGMFs model deflections as a collection of scattering events in random directions. Large scale simulations of EGMFs [53], as well as results from a recent semi-analytic analysis [54], conclude that deflections of proton UHECRs of energy E ≥ 40 EeV do not exceed 3° over 99% of the sky for $d \sim 100$ Mpc.

Magnetic deflection which is proportional to the charge is much larger for heavier UHECR nuclei and can completely wash out the directional correlation of UHECRs with their sources [55]. The composition of the UHECR sample we are considering here is at present uncertain but the anisotropies we would expect at lower energies if this dataset was composed of nuclei rather than nucleons have not been observed (see [56], [57]). Throughout most of this analysis we consider proton UHECRs. In order to bracket possible proton UHECR magnetic deflections we perform our analysis by averaging over angular bins in the range $3.9^\circ - 7.3^\circ$. We exclude the Galactic plane fom our analysis, $|b| \geq 12^\circ$, since UHECRs travelling through the Galactic plane may suffer strong deflections due to the magnetic field in the Galactic disc. In §3.2 we relax the assumption of nucleonic composition and investigate the effect that larger random deflections have on any correlation between the source population and the observed arrival direction distribution.

2.6 Correlation statistic

To detect any existing anisotropy signal we consider the counts-in-cells statistic X, proposed in [19], which characterises the correlation between the predicted and observed UHECR arrival direction distribution. In [19] X was shown to be more sensitive to the expected anisotropy signal than the angular power spectrum (e.g. [34], [58]) and the two point correlation function [59], which are other statistical measures commonly used in clustering analyses.

Let $\omega_{\mathrm{Auger,i}}$ be the exposure of PAO in bin i (see equation 2.1) and $\omega_{\mathrm{survey,i}}$ the weight imposed by the survey mask (given by [36], [37]):

$$\omega_{\mathrm{6dF,i}} = \begin{cases} 1 & \text{for } |b| > 10^\circ \text{ and } \delta \leq 0^\circ \\ 0 & \text{otherwise} \end{cases}$$

$$\omega_{\mathrm{PSCz,i}} = \begin{cases} 1 & \text{for } |b| > 10^\circ \\ 0 & \text{otherwise} \end{cases}$$

We define a combined weight:

$$\omega_{\mathrm{exposure,i}} = \omega_{\mathrm{Auger,i}} \cdot \omega_{\mathrm{survey,i}}. \tag{2.14}$$

We require that each of the quantities that go into our statistic are (a) weighted exactly once by the combined weight and (b) normalised so that each has a sum equal to the weighted sum of cosmic rays in the mask defined region. We restrict the analysis to the mask defined region by subjecting the number of cosmic rays in each bin i in the PAO dataset $N_{\mathrm{Auger,i}}$ to the survey mask:

$$N_{\mathrm{CR,i}} = \omega_{\mathrm{survey,i}} \cdot N_{\mathrm{Auger,i}}. \tag{2.15}$$

Note that $N_{\mathrm{Auger,i}}$, the observed number of cosmic rays, is naturally subject to $\omega_{\mathrm{Auger,i}}$ so we don't apply this weight again.

The number of survey galaxies visible by the PAO, $N_{\mathrm{gal,i}}$ is limited by the observatory's declination dependent exposure (equation 2.1). To account for this effect we subject each galaxy in bin i to the combined weight:

$$N_{\mathrm{gal,i}} = \omega_{\mathrm{exposure,i}} \cdot \sum_j \frac{\omega_{\mathrm{flux,j}}}{\psi(r_c)_j}, \tag{2.16}$$

where the sum is over the weighted contribution to the flux of each survey galaxy j in bin i. In the model where UHECR sources are correlated with galaxies in the nearby LSS, the expected number of cosmic rays $N_{\mathrm{M,i}}$ is simply $N_{\mathrm{gal,i}}$ normalised to the number of observed UHECRs according to condition (b):

$$N_{\mathrm{M,i}} = \frac{\sum_i N_{\mathrm{CR,i}}}{\sum_i N_{\mathrm{gal,i}}} \cdot N_{\mathrm{gal,i}}. \tag{2.17}$$

In an isotropic model the expected number of cosmic rays is given by:

$$N_{\mathrm{iso,i}} = \frac{\omega_{\mathrm{exposure,i}}}{n} \cdot \left(\frac{4\pi}{\int_0^\pi 2\pi \sin(\delta) \omega_{\mathrm{Auger}}(\delta)\, d\delta} \cdot \sum_j N_{\mathrm{Auger,j}} \right), \tag{2.18}$$

where n is the number of angular bins in the sky. The integral $\int_0^\pi 2\pi \sin(\delta) w(\delta)\, d\delta$ gives the total exposure of the PAO and hence $\frac{4\pi}{\int_0^\pi 2\pi \sin(\delta) w(\delta)\, d\delta}$ "unmasks" $N_{\mathrm{Auger,i}}$, i.e. the quantity in the brackets gives the number of cosmic rays that would have been observed if the PAO had had a uniform, full sky acceptance.

The statistic X is defined as:

$$X = \sum_i \frac{(N_{\rm CR,i} - N_{\rm iso,i})(N_{\rm M,i} - N_{\rm iso,i})}{N_{\rm iso,i}}. \tag{2.19}$$

We generate mock realisations of isotropic UHECR samples and correlate them with the galaxy maps to model the behaviour of X in an isotropic model. Similarly we create mock realisations of UHECRs that trace the local LSS by sampling from a Poisson distribution with a mean equal to the number of UHECRs expected to be detected per unit area at the PAO above energy E_f using the model of UHECR source distribution presented in §2.4. Finally we compute the statistic for the observed PAO UHECRs, and determine which of the 2 models of source distribution is preferred by the observed PAO UHECR dataset.

3 Results

The methodology presented in Section 2 was applied to the 69 UHECRs observed by the PAO with energy $E \geq 55$ EeV until the end of 2009 [18]. We perform our analysis by dividing the sky in equal area bins (counts-in-cells). The disadvantages of the counts-in-cells scheme are the effect of boundaries and the ability to arbitrarily choose the bin size. We deal with both these limitations by treating the size of the equal area bins as a free parameter in a range that covers expected random proton UHECR magnetic deflections (§3.1). In §3.2 we relax the assumption of proton UHECRs and investigate the sensitivity of our results to the magnitude of the magnetic deflection. We note that as explained in Section 2 we always mask out the galactic plane, as well the regions of the sky not covered by the galaxy survey, so the number of observed UHECRs that remain in the mask defined region is never 69 and depends on the survey used and the bin size considered. For simplicity we still write 69 events to specify the dataset that is being used.

3.1 Cross-correlation of UHECRs and nearby LSS

In figure 2 we show the distribution of sources of 55 EeV UHECR which follow the distribution of matter in the PSCz/6dF catalogues. To aid with illustration, we plot the model source distribution smeared with a 2 dimensional Gaussian filter with standard deviation $\sigma = 3^\circ, 7.2^\circ$, whereas throughout the rest of this work we have treated galaxies as discrete points. We plot the source distribution with the 69 observed PAO UHECRs superimposed in figure 3. In the maps of the PSCz one can see a very large contribution from the Virgo cluster ($l \sim -80^\circ, b \sim 75^\circ$), Hydra-Centaurus ($-60^\circ \leq l \leq 0^\circ, 0^\circ \leq b \leq 45^\circ$) and the Perseus-Pisces supercluster ($l \sim 140^\circ, b \sim -25^\circ$). In the maps of the 6dF there is a large excess as a result of flux from Hydra-Centaurus and the Shapley Concentration (centred at ($l \sim -50^\circ, b \sim 30^\circ$) at a distance ~ 200 Mpc). Note that we haven't masked with the PAO exposure in these plots. After doing so the relative weights of structures change so that for example Virgo no longer dominates in the PSCz derived model. Sky maps have been created using the HEALPix package [60].

Because the observed galaxy distribution is in the form of flux limited as opposed to volume limited samples, which would be more suitable for our analysis, we have weighted observed galaxies in the PSCz and 6dF with the inverse of the selection function $\psi(r_c)$ as

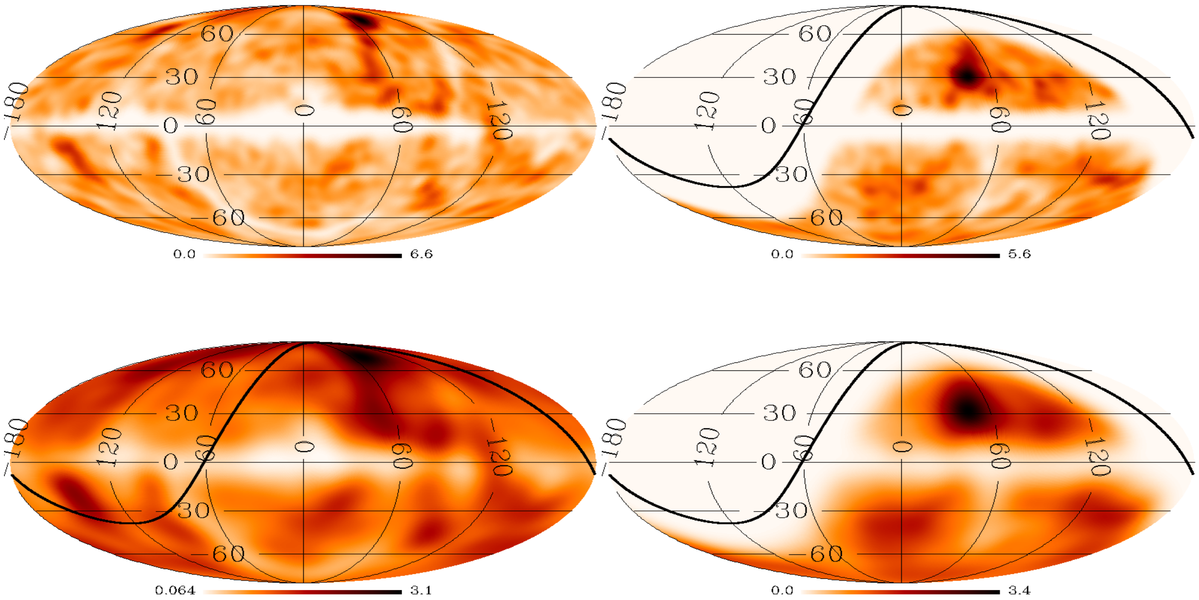

Figure 2: Maps of the predicted, local UHECR source density, in Galactic coordinates centred at the Galactic centre with the longitude l increasing anti-clockwise, derived from the PSCz (left) and 6dF (right) for UHECRs with final energy 55 EeV. The predicted source distribution has been smoothed with a Gaussian filter, with $\sigma = 3°$ (top row) and $\sigma = 7.2°$ (bottom row) for presentation purposes. The intensity at each point is normalised to its all sky average (half-sky for the 6dF). The PAO is sensitive to the part of the sky below the thick black line.

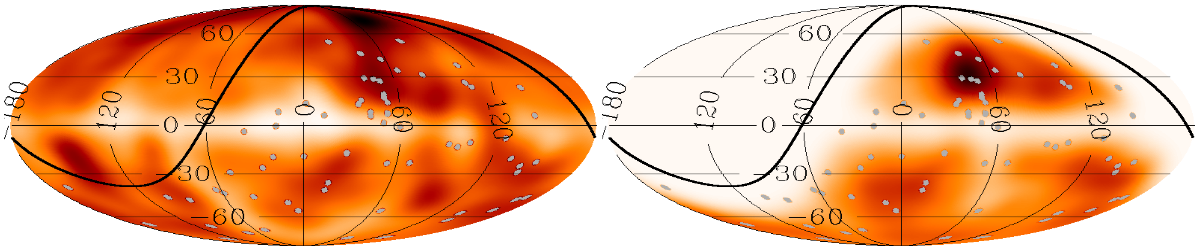

Figure 3: The predicted UHECR source density as in figure 2 above, but with the 69 PAO observed events superimposed (in grey). The PAO exposure has not been taken into account in this plot, hence visual inspection of correlations can be misleading. A statistical analysis as in §2.6 is required.

outlined in §2.4. There is a degree of uncertainty associated with this process, i.e. an error associated with the selection function which we have not taken into account, however the resulting flux contribution is likely to be close to its true value since matter in the universe is clustered.

In figures 4 and 5 we show the distribution of values that the statistic X takes in

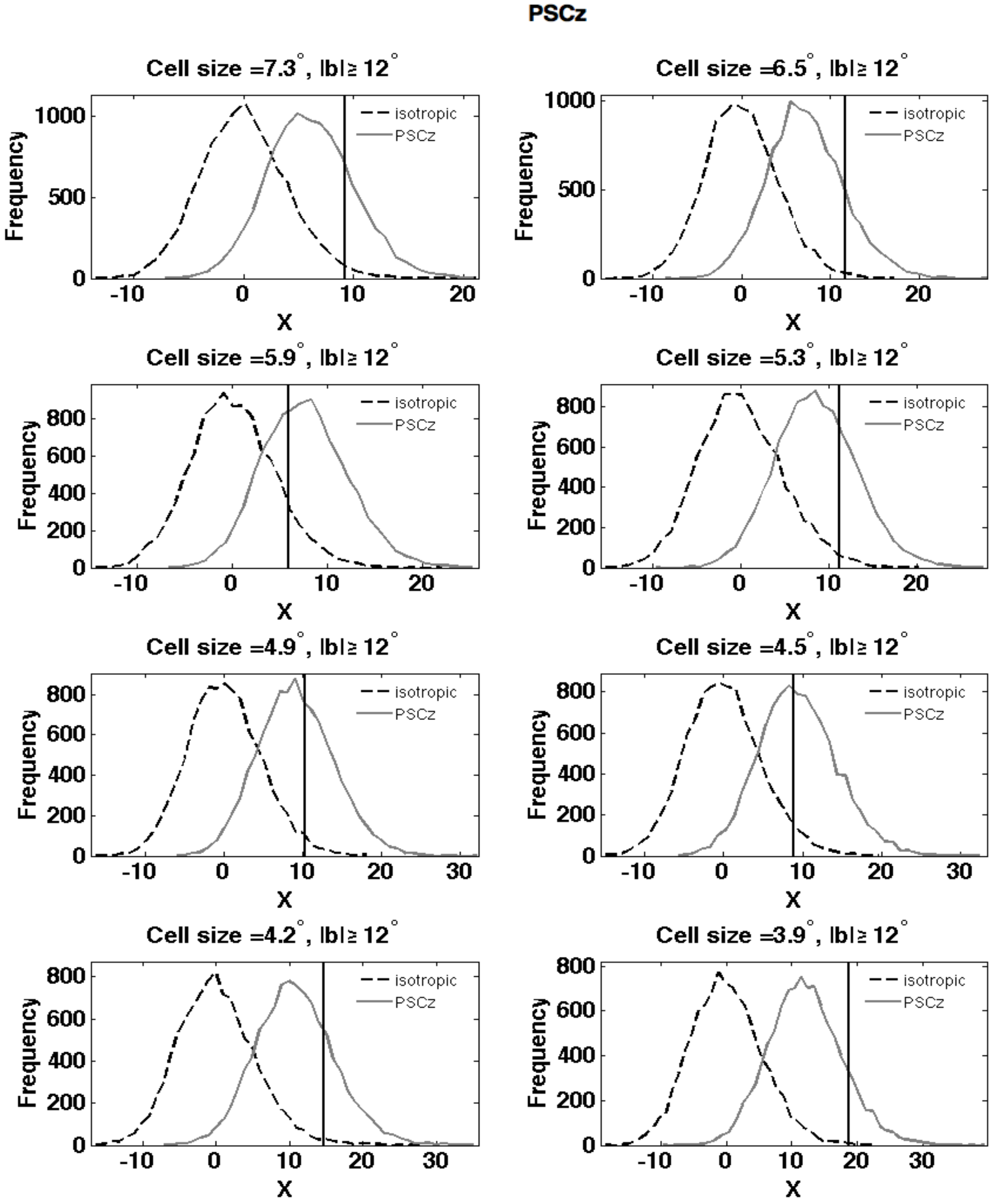
PSCz

Cell size =7.3°, |b|≥ 12°

Cell size =6.5°, |b|≥ 12°

Cell size =5.9°, |b|≥ 12°

Cell size =5.3°, |b|≥ 12°

Cell size =4.9°, |b|≥ 12°

Cell size =4.5°, |b|≥ 12°

Cell size =4.2°, |b|≥ 12°

Cell size =3.9°, |b|≥ 12°

Figure 4: The distribution of values of the correlation statistic X (equation (2.19)) in 10,000 mock realisations of a set of 69 UHECRs drawn from an isotropic distribution (dashed histograms) and from the predicted UHECR source distribution generated using the PSCz (solid histograms). The black vertical line indicates the value of X obtained for the 69 observed PAO events (X_{Auger}). Each subplot corresponds to a different cell size used for the counts-in-cells analysis in the range 7.3° (top left) to 3.9° (bottom right).

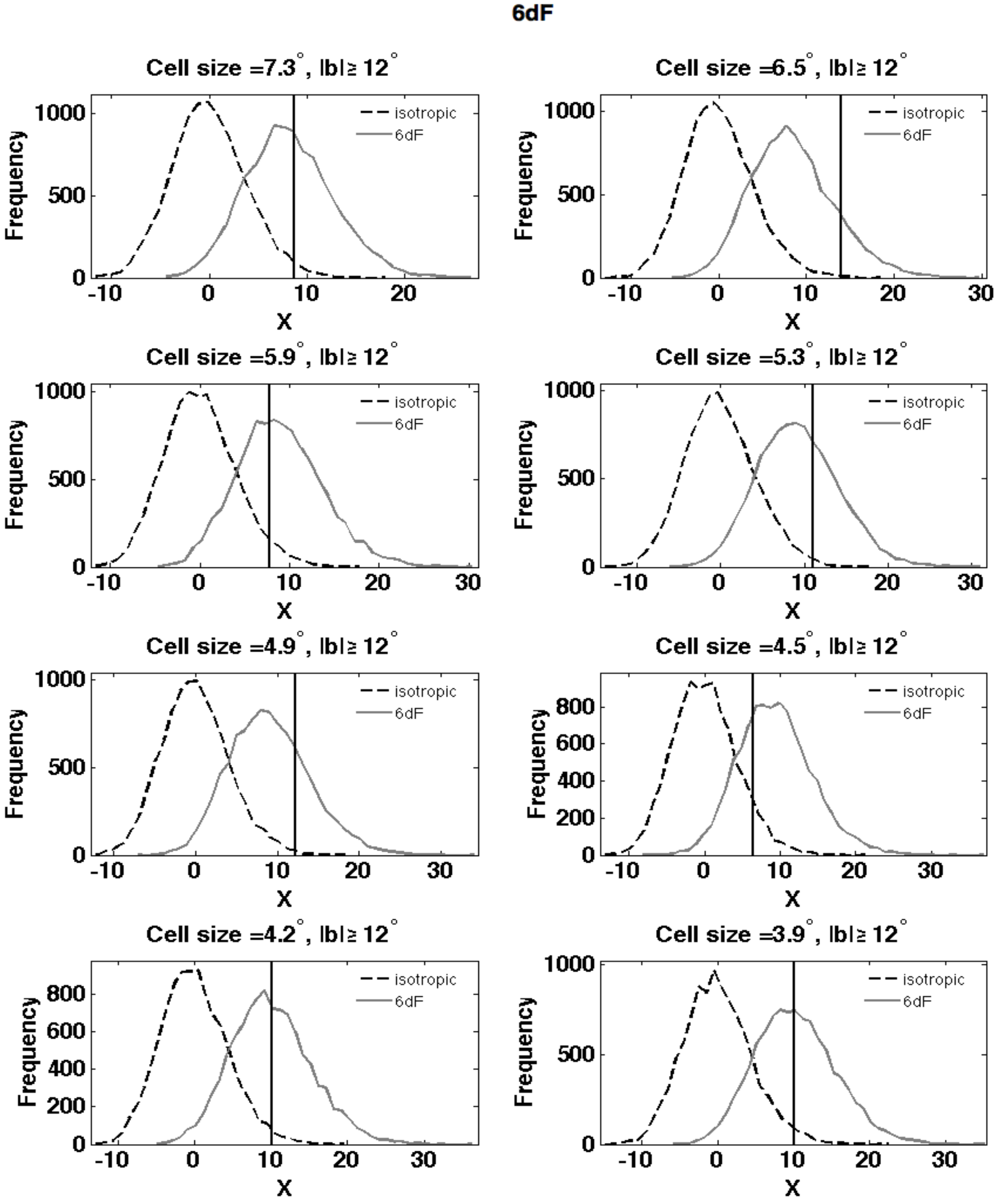

Figure 5: The same distributions as in figure 4 but using the 6dF catalogue.

10,000 mock realisations of 69 isotropically distributed UHECRs, as observed by the PAO (dashed histograms), and the distribution of values of X in 10,000 mock realisations of 55 EeV UHECR protons with sources drawn from the predicted UHECR source distribution in the case where UHECR sources follow the distribution of matter in the PSCz and 6dF catalogues respectively (solid histograms). The black vertical line in each subplot shows the value of X for the 69 observed PAO UHECRs assuming $E_f = 55$ EeV. Each subplot corresponds

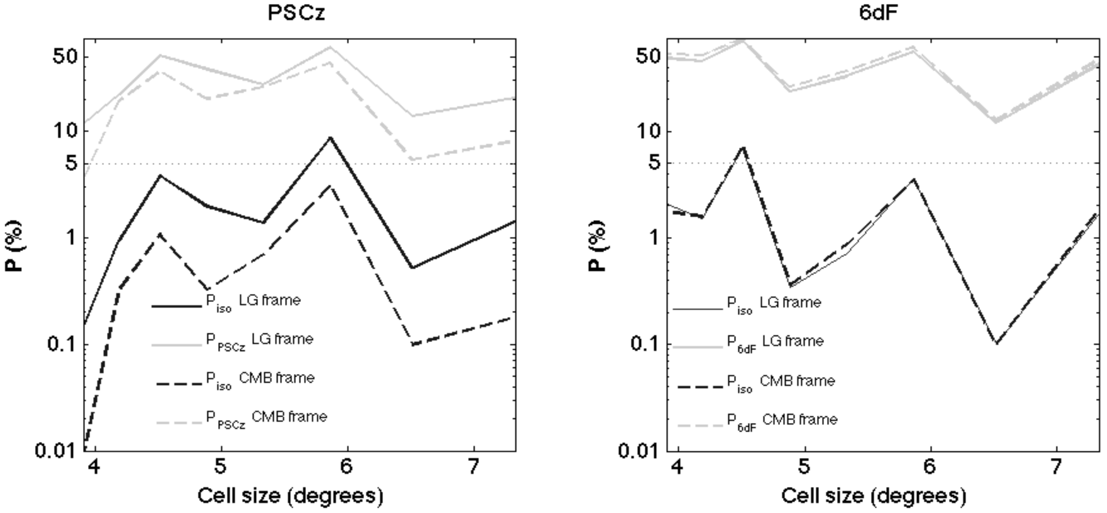

Figure 6: *Left:* $P_{\rm iso}$ - dark grey ($P_{\rm PSCz}$ - light grey), the percentage of realisations of an isotropic (correlated with LSS) UHECR source distribution in which the value of X was higher than the value of X obtained for the 69 observed PAO UHECRs, as a function of cell-size. *Right:* Same as on the *left* but using the 6dF survey. Results shown in solid lines are obtained using redshifts in the LG frame and in dashed lines with redshifts in the CMB frame. The horizontal dotted line shows the 95% confidence level.

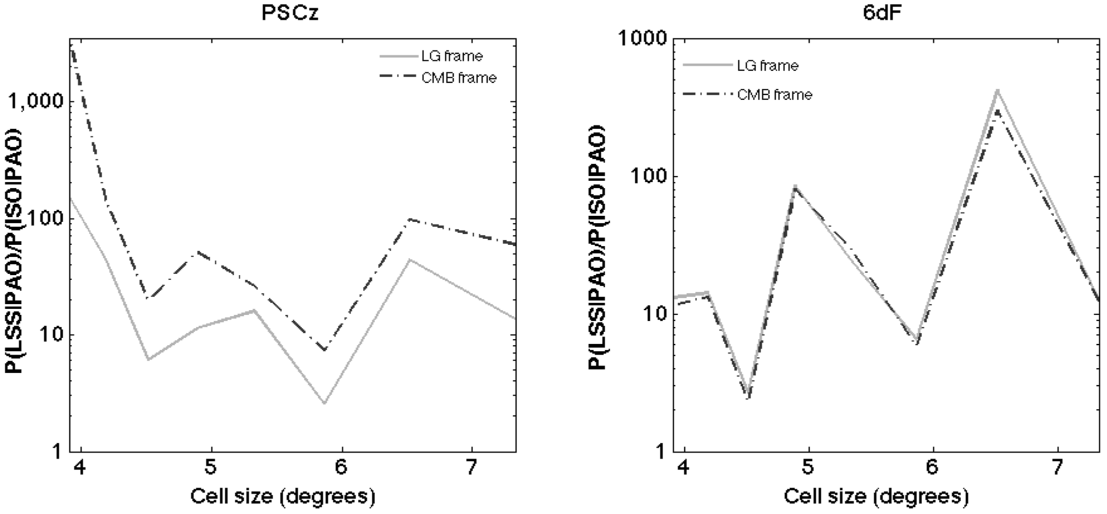

Figure 7: Ratio of the frequency with which the value of X obtained with the observed PAO UHECRs ($X_{\rm Auger}$) is obtained in each of the two models of UHECR source distribution we are considering (following LSS -LSS, isotropic -ISO) $\frac{P({\rm LSS}|{\rm PAO})}{P({\rm ISO}|{\rm PAO})}$ as a function of cell-size, for a model source distribution that follows the PSCz (left) and 6dF (right).

to a different cell-size in the range $7.3^\circ - 3.9^\circ$. We see that throughout the parameter space considered the observed PAO UHECRs are consistent with a source distribution correlated with nearby LSS whereas they have a value of X higher than in most mock isotropic UHECR realisations. We also see good agreement between the results obtained with the two galaxy

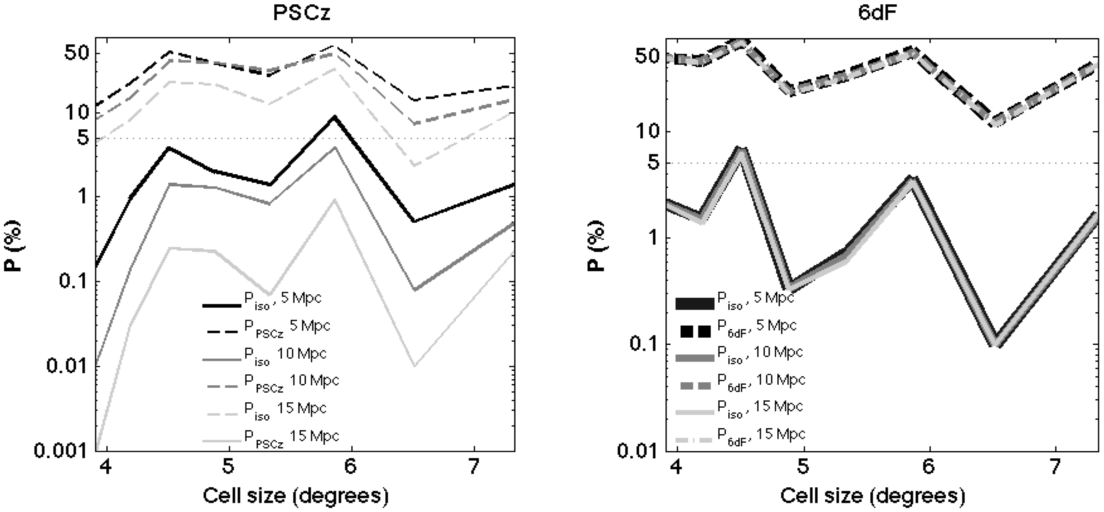

Figure 8: $P_{\rm iso}$ ($P_{\rm PSCz}$) - *Left*, $P_{\rm iso}$ ($P_{\rm 6dF}$) - *Right*, the percentage of realisations of an isotropic (correlated with LSS) UHECR source distribution in which the value of X was higher than the value of X obtained for the 69 observed PAO UHECRs, as a function of cell-size, after removing all galaxies within 5 (black), 10 (grey) and 15 Mpc (light grey).

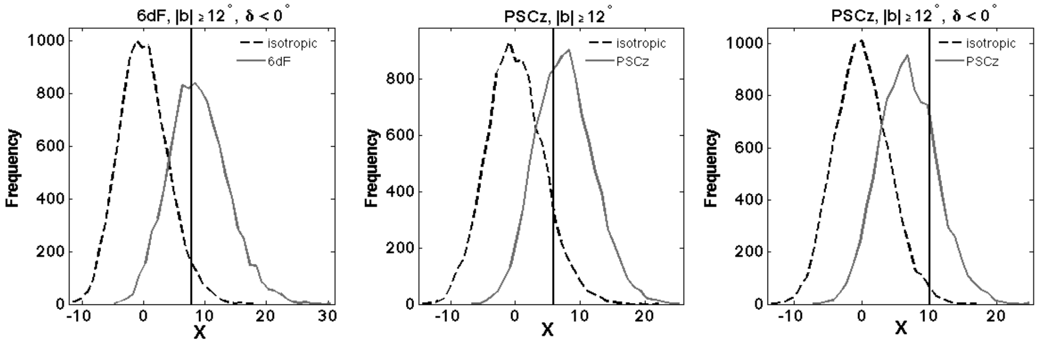

Figure 9: Distributions of the statistic X for realisations of UHECR sets with isotropic arrival directions (dashed histograms) and arrival directions correlated with the LSS (solid grey histograms). The value of X for the 69 observed PAO events is given by the black vertical line, for the 6dF (*left*), PSCz (*centre*), and PSCz only in the southern hemisphere (*right*). The plots shown are for cell size 5.9° × 5.9°.

surveys. Although the 6dF and PSCz samples are selected differently (near-infrared and far-infrared respectively) and the 6dF is deeper than the PSCz, they probe approximately the same large scale structure.

We quantify the significance of this result in figure 6, where we show the probability that a value of X greater than that obtained for the observed PAO UHECRs ($X_{\rm Auger}$) will be obtained in each of the models of UHECR source distribution ($P_{\rm iso}$ in the isotropic model and $P_{\rm PSCz}/P_{\rm 6dF}$ in the model where the UHECR sources are correlated with the local LSS), as a function of cell-size. Throughout the parameter space considered the observed PAO UHECRs exhibit a stronger correlation with nearby LSS than 90% of all isotropic mock realisations and are consistent with a source distribution that follows the distribution of matter in the PSCz/6dF surveys. In the same figure we show the results obtained using redshifts in the CMB as well as the LG frame. There is a larger spread between the predictions from the two reference frames for the PSCz catalogue, which is as expected, because the flux is dominated by more nearby structures.

There are differences between the model source distribution of ref. [19] derived from the PSCz catalogue and the PSCz derived model presented here, a main one being that they have considered a smoothed galaxy distribution whereas we have considered a distribution of point sources. When analysing the original 27 observed UHECRs using the PSCz to model the source distribution with comparable parameters, $E_f = 55$ EeV (57 EeV in [19]) and cell size $6.3^\circ \times 6.3^\circ$ ($6^\circ \times 6^\circ$ in [19]), we find $P_{\rm iso} = 1.03\%$ and $P_{\rm PSCz} = 8.7\%$, which are similar to their $P_I = 0.9\%$ and $P_{UB} = 3.8\%$.

Another way to quantify the significance of the results of figures 4 and 5 is to consider the frequencies with which the value of X obtained for the observed PAO UHECRs occurs in mock realisations of the two different models of UHECR source distribution. If the ratio of the likelihoods of the two model source distributions given the observed outcome $\frac{P(\text{Model 1}|\text{outcome})}{P(\text{Model 2}|\text{outcome})}$ is greater than 1 then Model 1 is preferred by the observed data. We show this ratio $\frac{P(\text{LSS source model is true}|X_{\rm Auger})}{P(\text{isotropic source model is true}|X_{\rm Auger})}$, hereafter $\frac{P(\text{LSS}|\text{PAO})}{P(\text{ISO}|\text{PAO})}$ separately for the two galaxy catalogues as a function of cell size in figure 7. The results shown in this plot vary considerably with cell size, but throughout the parameter space we have investigated there is a preference for a distribution of UHECR sources correlated with LSS, consistent with the results of figure 6.

Despite our treatment of our own peculiar velocity in space, there remain galaxies in the surveys we use to model the UHECR source distribution which appear to be much closer to the earth than they are in reality and others that appear to have a negative redshift as a result of their own peculiar motions. To deal with this we assign galaxies whose distances are known from independent measurements their measured distances, instead of converting them from redshifts and we remove from the model of UHECR source distribution all galaxies that are (or appear to be) within less than 5 Mpc comoving. In order to test the robustness of our results to this cut we consider how cuts of 10 and 15 Mpc affect our results. In figure 8 we plot the quantities $P_{\rm iso}$ and $P_{\rm PSCz}/P_{\rm 6dF}$ (defined earlier on in this section) after removing all galaxies within 5, 10 and 15 Mpc form the UHECR source model as a function of cell size. The effect of this cut is almost negligible in the 6dF analysis because it is a slightly deeper survey and flux from the nearest galaxies does not dominate the expected flux on earth. The results obtained with the PSCz are more sensitive to this cut, but our conclusions are robust with respect to this cut since in all cases and for both surveys the PAO observed UHECRs have a higher value of X than 90% of all isotropic mock realisations and are consistent with a distribution of sources which follows LSS.

In figure 9 we show the results of the correlation analysis performed using the 6dF survey next to the same results for the PSCz, as well as the results of the analysis performed with the PSCz survey but restricted to the Southern hemisphere. This allows for a direct comparison between the results of the two surveys since we confine the analysis to the part of the sky that they are both sensitive to. Again we see good agreement between the two surveys and the observed PAO UHECRs are consistent with a distribution of sources correlated with nearby galaxies.

There is a 23% systematic uncertainty in the energy determination of the primary particles detected at PAO which introduces an error to our results. We have investigated how

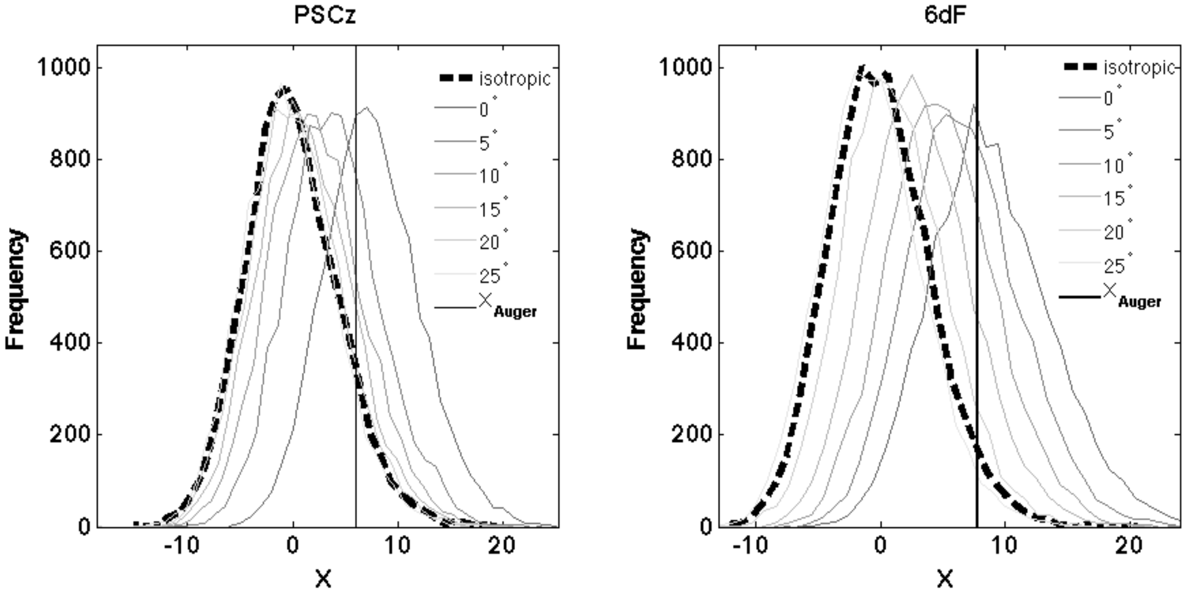

Figure 10: The distribution of values of X in 10,000 realisations of 69 isotropic UHECR events (dashed histogram) and 69 UHECRs whose sources are in local galaxies (solid histograms) with simulated magnetic deflections (PSCz-*left subplot* and 6dF-*right subplot*). In each solid histogram the UHECRs arrive on Earth with a mean position centred at the source's true position and random angular deflections with amplitude σ given in the legend.

this uncertainty affects our results and found that they are robust to this uncertainty, i.e. changing E_f in our models by 23% does not change our conclusions.

3.2 Magnetic deflection

We investigate the dependence of our results on the amplitude of the magnetic deflections suffered by UHECRs during their propagation. If UHECRs are Fe nuclei as some experimental data suggest [18], average deflections are likely to be of the order of 20°. The results obtained in this section are relevant to protons and Fe nuclei which are attenuated over similar distances at energy above ~ 40 EeV but not to intermediate mass nuclei which have a much shorter mean free path at this energy range (see for example [61]).

We generate mock realisations in which UHECRs suffer simulated magnetic deflections d in the range $5^\circ - 25^\circ$ and determine the range of deflection angles for which a correlation with the source population can be established. We also compare these model distributions to the 69 observed PAO UHECRs. We simulate random magnetic deflections in the arrival directions of UHECRs by allowing for a shift in their positions with respect to the position of their sources. We do so using a 2 dimensional Gaussian function with a width d centred at the position of the source and according to it we generate randomly oriented angular displacements for each UHECR in each mock realisation.

In figure 10 we show the distribution of values of X obtained for mock UHECRs, whose sources are nearby galaxies, and which have suffered magnetic deflections in the range $0^\circ - 25^\circ$. We find that even if the sources of the UHECRs are correlated with nearby galaxies (as the ones in our model) increasing the deflection angle dilutes the correlation signal and for a dataset of 69 events the correlation with the source population is wiped out by deflections greater than $\sim 20^\circ$. We also show the value of X obtained for the 69 PAO observed UHECRs, X_{Auger}. At present, given the value of X_{Auger} obtained, we cannot exclude deflections of more than 20°. With a larger dataset, if the correlation of observed UHECRs with LSS persists, we will be able to exclude large deflections and hence a heavy composition.

4 Discussion and Conclusions

We have used the set of 69 observed PAO UHECRs with energy greater than 55 EeV to assess whether their arrival directions are correlated with nearby galaxies. We model the UHECR source distribution using the 6dF and PSCz galaxy surveys, taking into account the UHECR flux suppression due to energy losses during particle propagation and the non-uniform PAO exposure. We have shown that the probability that the observed UHECRs are consistent with an isotropic distribution is less than 5% for most of the parameter space considered.

The analysis performed with the 6dF, which is being used here for the first time to model the local UHECR source distribution agrees well with that obtained with the PSCz despite the two surveys having different median depths and fields of view. The results obtained here are in agreement with those of other studies such as [24] in that the observed UHECRs exhibit an anisotropy which is consistent with the distribution of nearby galaxies, although our results are not directly comparable due to the different statistical approaches and UHECR source models used.

In this work we have taken a Frequentist approach to the long standing question of the origin of UHECRs, as we consider it the most straightforward approach with the smallest number of assumptions regarding the source population. Other authors have taken a Bayesian approach to the question [30], and despite using different models of source population they have obtained results that are qualitatively similar to the ones obtained in this and similar analyses, namely that the UHECRs observed to date (or at least a significant fraction of them) are inconsistent with an isotropic distribution of sources and consistent with models in which the sources are luminous galaxies in the nearby universe.

Our analysis has been performed with two galaxy surveys which have been carried out using different selection criteria and hence probe different astrophysical populations. Observing a correlation with a specific astrophysical population does not constitute proof that the sources of UHECRs are members of that population, as matter in the universe is clustered and different astrophysical populations are correlated with each other. The confidence intervals with which we can exclude isotropy using the two surveys are comparable which exhibits the robustness of our results. With a larger UHECR dataset one may hope to distinguish between different source populations, if the strength of EGMFs is not too large and the composition is nucleonic.

We note that in this work we have only considered the case of faint sources which is well motivated in the absence of significant small scale clustering (repeaters) in the dataset.

We have excluded the Galactic plane throughout our analysis, both due to the incompleteness of the galaxy surveys and because UHECRs travelling through the Galactic plane are likely to suffer significant deflections due to the Galactic disc's magnetic field. We have attempted to set a limit on the deflection suffered by the PAO UHECRs since the strength of Galactic magnetic fields and EGMFs as well as the composition of the UHECRs remain loosely constrained. We have shown that the arrival direction distribution of UHECRs which have been deflected by more than 20° would be difficult to distinguish from an isotropically produced dataset with a dataset of ~ 70 events. With the present dataset we cannot exclude deflections above 20° but with a larger dataset it will be possible to do so if the observed correlation with LSS persists. Excluding large deflections would suggest the absence of Fe nuclei for most models of EGMFs.

5 Acknowledgements

FO and ST acknowledge the support of UCL's Institute of Origins. AC acknowledges support from the Royal Society for an International Incoming Fellowship. FBA acknowledges the support of the Royal Society via a Royal Society URF award. OL acknowledges support from a Royal Society Wolfson Research Merit Award, a Leverhulme Senior Research Fellowship and an Advanced Grant from the European Research Council.

Bibliography

[1] P. Bhattacharjee, *Origin and propagation of extremely high energy cosmic rays*, *Physics Reports* **327** (Mar., 2000) 109–247, [astro-ph/9811011].

[2] M. Nagano and A. A. Watson, *Observations and implications of the ultrahigh-energy cosmic rays*, *Reviews of Modern Physics* **72** (July, 2000) 689–732.

[3] A. M. Hillas, *The Origin of Ultra-High-Energy Cosmic Rays*, *Annual Review of Astronomy and Astrophysics* **22** (1984) 425–444.

[4] K. Greisen, *End to the Cosmic-Ray Spectrum?*, *Physical Review Letters* **16** (Apr., 1966) 748–750.

[5] G. T. Zatsepin and V. A. Kuz'min, *Upper Limit of the Spectrum of Cosmic Rays*, *Soviet Journal of Experimental and Theoretical Physics Letters* **4** (Aug., 1966) 78.

[6] J. Abraham, P. Abreu, M. Aglietta, E. J. Ahn, D. Allard, J. Allen, J. Alvarez-Muñiz, M. Ambrosio, L. Anchordoqui, S. Andringa, and et al., *Measurement of the energy spectrum of cosmic rays above 10^{18} eV using the Pierre Auger Observatory*, *Physics Letters B* **685** (Mar., 2010) 239–246, [arXiv:1002.1975].

[7] J. e. a. Abraham, *Observation of the Suppression of the Flux of Cosmic Rays above $4{\times}10^{19} eV$*, *Physical Review Letters* **101** (Aug., 2008) 061101, [arXiv:0806.4302].

[8] G. B. Thomson, *Results from the Telescope Array Experiment*, *ArXiv e-prints* (Oct., 2010) [arXiv:1010.5528].

[9] K. V. Ptitsyna and S. V. Troitsky, *PHYSICS OF OUR DAYS Physical conditions in potential accelerators of ultra-high-energy cosmic rays: updated Hillas plot and radiation-loss constraints*, *Physics Uspekhi* **53** (Oct., 2010) 691–701, [arXiv:0808.0367].

[10] R. Abbasi, Y. Abdou, T. Abu-Zayyad, M. Ackermann, J. Adams, J. A. Aguilar, M. Ahlers, D. Altmann, K. Andeen, J. Auffenberg, and et al., *An absence of neutrinos associated with cosmic-ray acceleration in γ-ray bursts*, *Nature* **484** (Apr., 2012) 351–354, [arXiv:1204.4219].

[11] A. Dar, *Neutrinos And Cosmic Rays From Gamma Ray Bursts*, *ArXiv e-prints* (May, 2012) [arXiv:1205.3479].

[12] H.-N. He, R.-Y. Liu, X.-Y. Wang, S. Nagataki, K. Murase, and Z.-G. Dai, *Icecube Nondetection of Gamma-Ray Bursts: Constraints on the Fireball Properties*, *The Astrophysical Journal* **752** (June, 2012) 29, [arXiv:1204.0857].

[13] E. Waxman, K. B. Fisher, and T. Piran, *The Signature of a Correlation between Cosmic-Ray Sources above 10 19 eV and Large-Scale Structure*, *The Astrophysical Journal* **483** (July, 1997) 1, [astro-ph/9604005].

[14] J. Abraham, P. Abreu, M. Aglietta, E. J. Ahn, D. Allard, I. Allekotte, J. Allen, J. Alvarez-Muñiz, M. Ambrosio, L. Anchordoqui, and et al., *Measurement of the Depth of Maximum of Extensive Air Showers above* 10^{18} *eV*, *Physical Review Letters* **104** (Mar., 2010) 091101, [arXiv:1002.0699].

[15] The Telescope Array Collaboration, *Cosmic Ray in the Northern Hemisphere: Results from the Telescope Array Experiment*, *ArXiv e-prints* (2011) [arXiv:1110.0133].

[16] P. Sokolsky and for the HiRes Collaboration, *Final Results from the High Resolution Fly's Eye (HiRes) Experiment*, *ArXiv e-prints* (Oct., 2010) [arXiv:1010.2690].

[17] E. Waxman, *High energy cosmic ray and neutrino astronomy*, *ArXiv e-prints* (Jan., 2011) [arXiv:1101.1155].

[18] The Pierre Auger Collaboration, P. Abreu, M. Aglietta, E. J. Ahn, D. Allard, I. Allekotte, J. Allen, J. Alvarez Castillo, J. Alvarez-Muñiz, M. Ambrosio, and et al., *Update on the correlation of the highest energy cosmic rays with nearby extragalactic matter*, *Astroparticle Physics* **34** (Dec., 2010) 314–326, [arXiv:1009.1855].

[19] T. Kashti and E. Waxman, *Searching for a correlation between cosmic-ray sources above* 10^{19} *eV and large scale structure*, *Journal of Cosmology and Astro-Particle Physics* **5** (May, 2008) 006, [arXiv:0801.4516].

[20] A. A. Berlind, G. R. Farrar, and I. Zaw, *Correlations Between Ultrahigh Energy Cosmic Rays and Infrared-luminous Galaxies*, *The Astrophysical Journal* **716** (June, 2010) 914–917, [arXiv:0904.4276].

[21] H. Takami, H. Yoshiguchi, and K. Sato, *Propagation of Ultra-High-Energy Cosmic Rays above* 10^{19} *eV in a Structured Extragalactic Magnetic Field and Galactic Magnetic Field*, *The Astrophysical Journal* **639** (Mar., 2006) 803–815, [astro-ph/0506203].

[22] A. Cuoco, R. D'Abrusco, G. Longo, G. Miele, and P. D. Serpico, *The footprint of large scale cosmic structure on the ultrahigh energy cosmic ray distribution*, *Journal of Cosmology and Astro-Particle Physics* **1** (Jan., 2006) 9, [astro-ph/0510765].

[23] H. B. J. Koers and P. Tinyakov, *Testing large-scale (an)isotropy of ultra-high energy cosmic rays*, *Journal of Cosmology and Astroparticle Physics* **4** (Apr., 2009) 3, [arXiv:0812.0860].

[24] R. U. Abbasi, T. Abu-Zayyad, M. Allen, and The High Resolution Fly's Eye Collaboration, *Analysis of Large-scale Anisotropy of Ultra-high Energy Cosmic Rays in HiRes Data*, *The Astrophysical Journal Letters* **713** (Apr., 2010) L64–L68, [arXiv:1002.1444].

[25] The Pierre Auger Collaboration: J. Abraham, P. Abreu, M. Aglietta, C. Aguirre, E. J. Ahn, D. Allard, I. Allekotte, J. Allen, J. Alvarez-Muñiz, M. Ambrosio, and et al., *Astrophysical Sources of Cosmic Rays and Related Measurements with the Pierre Auger Observatory*, *ArXiv e-prints* (June, 2009) [arXiv:0906.2347].

[26] The Pierre Auger Collaboration, J. Abraham, P. Abreu, M. Aglietta, C. Aguirre, D. Allard, I. Allekotte, J. Allen, P. Allison, C. Alvarez, and et al., *Correlation of the Highest-Energy Cosmic Rays with Nearby Extragalactic Objects*, *Science* **318** (Nov., 2007) 938–, [arXiv:0711.2256].

[27] Pierre Auger Collaboration, J. Abraham, P. Abreu, M. Aglietta, C. Aguirre, D. Allard, I. Allekotte, J. Allen, P. Allison, J. Alvarez-Muñiz, and et al., *Correlation of the highest-energy cosmic rays with the positions of nearby active galactic nuclei*, *Astroparticle Physics* **29** (Apr., 2008) 188–204, [arXiv:0712.2843].

[28] M. R. George, A. C. Fabian, W. H. Baumgartner, R. F. Mushotzky, and J. Tueller, *On active*

galactic nuclei as sources of ultra-high energy cosmic rays, *Monthly Notices of the RAS* **388** (July, 2008) L59–L63, [arXiv:0805.2053].

[29] A. Pe'Er, K. Murase, and P. Mészáros, *Radio-quiet active galactic nuclei as possible sources of ultrahigh-energy cosmic rays*, *Physical Review D* **80** (Dec., 2009) 123018, [arXiv:0911.1776].

[30] L. J. Watson, D. J. Mortlock, and A. H. Jaffe, *A Bayesian analysis of the 27 highest energy cosmic rays detected by the Pierre Auger Observatory*, *Monthly Notices of the RAS* **418** (Nov., 2011) 206–213, [arXiv:1010.0911].

[31] P. G. Tinyakov and I. I. Tkachev, *BL Lacertae are Probable Sources of the Observed Ultrahigh Energy Cosmic Rays*, *Soviet Journal of Experimental and Theoretical Physics Letters* **74** (Nov., 2001) 445–448, [astro-ph/0102476].

[32] J. Tueller, W. H. Baumgartner, C. B. Markwardt, G. K. Skinner, R. F. Mushotzky, M. Ajello, S. Barthelmy, A. Beardmore, W. N. Brandt, D. Burrows, G. Chincarini, S. Campana, J. Cummings, G. Cusumano, P. Evans, E. Fenimore, N. Gehrels, O. Godet, D. Grupe, S. Holland, J. Kennea, H. A. Krimm, M. Koss, A. Moretti, K. Mukai, J. P. Osborne, T. Okajima, C. Pagani, K. Page, D. Palmer, A. Parsons, D. P. Schneider, T. Sakamoto, R. Sambruna, G. Sato, M. Stamatikos, M. Stroh, T. Ukwata, and L. Winter, *The 22 Month Swift-BAT All-Sky Hard X-ray Survey*, *The Astrophysical Journal Supplement Series* **186** (Feb., 2010) 378–405, [arXiv:0903.3037].

[33] J. Abraham, M. Aglietta, I. C. Aguirre, M. Albrow, D. Allard, I. Allekotte, P. Allison, J. Alvarez Muñiz, M. G. Do Amaral, M. Ambrosio, and et al., *Properties and performance of the prototype instrument for the Pierre Auger Observatory*, *Nuclear Instruments and Methods in Physics Research A* **523** (May, 2004) 50–95.

[34] P. Sommers, *Cosmic ray anisotropy analysis with a full-sky observatory*, *Astroparticle Physics* **14** (Jan., 2001) 271–286, [astro-ph/0004016].

[35] The Pierre Auger Collaboration, P. Abreu, M. Aglietta, E. J. Ahn, I. F. M. Albuquerque, D. Allard, I. Allekotte, J. Allen, P. Allison, J. Alvarez Castillo, and et al., *The Pierre Auger Observatory I: The Cosmic Ray Energy Spectrum and Related Measurements*, *ArXiv e-prints* (July, 2011) [arXiv:1107.4809].

[36] D. H. Jones, M. A. Read, W. Saunders, M. Colless, T. Jarrett, Q. A. Parker, A. P. Fairall, T. Mauch, E. M. Sadler, F. G. Watson, D. Burton, L. A. Campbell, P. Cass, S. M. Croom, J. Dawe, K. Fiegert, L. Frankcombe, M. Hartley, J. Huchra, D. James, E. Kirby, O. Lahav, J. Lucey, G. A. Mamon, L. Moore, B. A. Peterson, S. Prior, D. Proust, K. Russell, V. Safouris, K. Wakamatsu, E. Westra, and M. Williams, *The 6dF Galaxy Survey: final redshift release (DR3) and southern large-scale structures*, *MNRAS* **399** (Oct., 2009) 683–698, [arXiv:0903.5451].

[37] W. Saunders, W. J. Sutherland, S. J. Maddox, O. Keeble, S. J. Oliver, M. Rowan-Robinson, R. G. McMahon, G. P. Efstathiou, H. Tadros, S. D. M. White, C. S. Frenk, A. Carramiñana, and M. R. S. Hawkins, *The PSCz catalogue*, *MNRAS* **317** (Sept., 2000) 55–63, [astro-ph/0001117].

[38] S. L. Dubovsky, P. G. Tinyakov, and I. I. Tkachev, *Statistics of Clustering of Ultrahigh Energy Cosmic Rays and the Number of Their Sources*, *Physical Review Letters* **85** (Aug., 2000) 1154–1157, [astro-ph/0001317].

[39] Z. Fodor and S. D. Katz, *Ultrahigh energy cosmic rays from compact sources*, *Physical Review D* **63** (Jan., 2001) 023002, [hep-ph/0007158].

[40] G. Cavallo, *On the sources of ultra-high energy cosmic rays*, *Astronomy and Astrophysics* **65** (May, 1978) 415–419.

[41] G. E. Romero, J. A. Combi, S. E. Perez Bergliaffa, and L. A. Anchordoqui, *Centaurus A as a source of extragalactic cosmic rays with arrival energies well beyond the GZK cutoff*,

Astroparticle Physics **5** (Oct., 1996) 279–283, [gr-qc/9511031].

[42] L. A. Anchordoqui, H. Goldberg, and T. J. Weiler, *Auger Test of the Cen A Model of Highest Energy Cosmic Rays*, *Physical Review Letters* **87** (Aug., 2001) 081101, [astro-ph/0103043].

[43] J. N. Bahcall and E. Waxman, *Ultra-High-Energy Cosmic Rays May Come from Clustered Sources*, *The Astrophysical Journal* **542** (Oct., 2000) 542–547, [hep-ph/9912326].

[44] R. Blandford and D. Eichler, *Particle acceleration at astrophysical shocks: A theory of cosmic ray origin*, *Physics Reports* **154** (Oct., 1987) 1–75.

[45] A. Achterberg, Y. A. Gallant, J. G. Kirk, and A. W. Guthmann, *Particle acceleration by ultrarelativistic shocks: theory and simulations*, *Monthly Notices of the RAS* **328** (Dec., 2001) 393–408, [astro-ph/0107530].

[46] Z. Fodor, S. D. Katz, A. Ringwald, and H. Tu, *Bounds on the cosmogenic neutrino flux*, *Journal of Cosmology and Astro-Particle Physics* **11** (Nov., 2003) 15, [hep-ph/0309171].

[47] P. Erdoğdu, O. Lahav, J. P. Huchra, M. Colless, R. M. Cutri, E. Falco, T. George, T. Jarrett, D. H. Jones, L. M. Macri, J. Mader, N. Martimbeau, M. A. Pahre, Q. A. Parker, A. Rassat, and W. Saunders, *Reconstructed density and velocity fields from the 2MASS Redshift Survey*, *Monthly Notices of the RAS* **373** (Nov., 2006) 45–64, [astro-ph/0610005].

[48] S. Courteau and S. van den Bergh, *The Solar Motion Relative to the Local Group*, *Astronomical Journal* **118** (July, 1999) 337–345, [astro-ph/9903298].

[49] N. Jarosik, C. L. Bennett, J. Dunkley, B. Gold, M. R. Greason, M. Halpern, R. S. Hill, G. Hinshaw, A. Kogut, E. Komatsu, D. Larson, M. Limon, S. S. Meyer, M. R. Nolta, N. Odegard, L. Page, K. M. Smith, D. N. Spergel, G. S. Tucker, J. L. Weiland, E. Wollack, and E. L. Wright, *Seven-year Wilkinson Microwave Anisotropy Probe (WMAP) Observations: Sky Maps, Systematic Errors, and Basic Results*, *The Astrophysical Journal Supplement Series* **192** (Feb., 2011) 14, [arXiv:1001.4744].

[50] P. P. Kronberg, *Extragalactic magnetic fields*, *Reports on Progress in Physics* **57** (Apr., 1994) 325–382.

[51] J. P. Vallee, *Observations of the Magnetic Fields Inside and Outside the Milky Way, Starting with Globules (˜ 1 parsec), Filaments, Clouds, Superbubbles, Spiral Arms, Galaxies, Superclusters, and Ending with the Cosmological Universe's Background Surface (at ˜ 8 Teraparsecs)*, *Fundamental Cosmic Physics* **19** (1997) 1–89.

[52] E. Waxman and J. Miralda-Escude, *Images of Bursting Sources of High-Energy Cosmic Rays: Effects of Magnetic Fields*, *The Astrophysical Journal Letters* **472** (Dec., 1996) L89, [astro-ph/9607059].

[53] K. Dolag, D. Grasso, V. Springel, and I. Tkachev, *Constrained simulations of the magnetic field in the local Universe and the propagation of ultrahigh energy cosmic rays*, *Journal of Cosmology and Astroparticle Physics* **1** (Jan., 2005) 9, [astro-ph/0410419].

[54] K. Kotera and M. Lemoine, *Optical depth of the Universe to ultrahigh energy cosmic ray scattering in the magnetized large scale structure*, *Physical Review D* **77** (June, 2008) 123003, [arXiv:0801.1450].

[55] R. Aloisio, V. Berezinsky, and A. Gazizov, *Ultra High Energy Cosmic Rays: The disappointing model*, *ArXiv e-prints* (July, 2009) [arXiv:0907.5194].

[56] M. Lemoine and E. Waxman, *Anisotropy vs chemical composition at ultra-high energies*, *Journal of Cosmology and Astroparticle Physics* **11** (Nov., 2009) 9, [arXiv:0907.1354].

[57] The Pierre Auger Collaboration, P. Abreu, M. Aglietta, E. J. Ahn, I. F. M. Albuquerque, D. Allard, I. Allekotte, J. Allen, P. Allison, J. Alvarez Castillo, and et al., *Anisotropy and chemical composition of ultra-high energy cosmic rays using arrival directions measured by the*

Pierre Auger Observatory, *ArXiv e-prints* (June, 2011) [arXiv:1106.3048].

[58] M. Tegmark, D. H. Hartmann, M. S. Briggs, and C. A. Meegan, *The Angular Power Spectrum of BATSE 3B Gamma-Ray Bursts*, *The Astrophysical Journal* **468** (Sept., 1996) 214, [astro-ph/9510129].

[59] M. Kachelrieß and D. V. Semikoz, *Clustering of ultra-high energy cosmic ray arrival directions on medium scales*, *Astroparticle Physics* **26** (Aug., 2006) 10–15, [astro-ph/0512498].

[60] K. M. Górski, E. Hivon, A. J. Banday, B. D. Wandelt, F. K. Hansen, M. Reinecke, and M. Bartelmann, *HEALPix: A Framework for High-Resolution Discretization and Fast Analysis of Data Distributed on the Sphere*, *The Astrophysical Journal* **622** (Apr., 2005) 759–771, [astro-ph/0409513].

[61] D. Allard, E. Parizot, A. V. Olinto, E. Khan, and S. Goriely, *UHE nuclei propagation and the interpretation of the ankle in the cosmic-ray spectrum*, *Astronomy and Astrophysics* **443** (Dec., 2005) L29–L32, [astro-ph/0505566].